Acta Cryst E CRYSTALLOGRAPHIC COMMUNICATIONS

ISSN 2056-9890

Synthesis and structure of 9-methyl-1,10-dihydropyrazolo[3,4-*a*]carbazole

M. Sridharan,[a]* Aravazhi Amalan Thiruvalluvar[b]* and B. M. Rajesh[c]

[a]Department of Chemistry, RV College of Engineering, Bangalore 560 059, Karnataka, India, [b]Principal (Retired), 63 Shanthi Nagar, 5th Street, Nanjikottai Road, Thanjavur 613 006, Tamilnadu, India, and [c]Department of Physics, RV College of Engineering, Bangalore 560 059, Karnataka, India. *Correspondence e-mail: sridharanm@rvce.edu.in, thiruvalluvar.a@gmail.com

Received 13 January 2026
Accepted 19 January 2026

Edited by W. T. A. Harrison, University of Aberdeen, United Kingdom

Keywords: crystal structure; carbazole; Hirshfeld surface; N—H···N hydrogen bonding; C—H···π contact.

CCDC reference: 2524177

Supporting information: this article has supporting information at journals.iucr.org/e

The title carbazole derivative, $C_{14}H_{11}N_3$, was prepared by reacting 1-hydroxy-8-methyl-9*H*-carbazole-2-carbaldehyde with hydrazine hydrate. In the solid state, the fused-ring system is slightly puckered, the dihedral angle between the planes of the outer rings being 2.24 (7)°. In the crystal, molecules are linked by $\{N-H\}_2\cdots N$ hydrogen bonds to generate [010] chains, and weak C—H···π contacts consolidate the structure. A Hirshfeld surface analysis indicates that the most important contributions to the crystal packing are from H···H (43.1%), C···H/H···C (36.8%) and N···H/H···N (15.3%) interactions.

1. Chemical context

Carbazoles are tricyclic aromatic heterocycles that have attracted significant attention due to their presence in natural products and their wide-ranging biological activities. Synthetic methodologies to access carbazoles and their fused-ring derivatives include direct annulation, cyclization reactions and transition-metal catalysis (Knölker & Reddy, 2002). Linear and angular fused carbazoles, such as pyrido-, pyrazolo-, pyrimido- and pyridazinocarbazoles, possess pharmacological applications, including antitumour and anti-HIV activities, as well as an ability to act as DNA intercalating agents (Kumar *et al.*, 2023; El-Essawy & Odah, 2024). Among these, pyrazolo-annulated heterocycles like pyrazolopyridopyrimidines stand out for their structural complexity, containing five N atoms and three fused rings, which combine the properties of pyrazole, pyridine and pyrimidine (Iorkula *et al.*, 2025). Beyond therapeutic applications, carbazole derivatives have emerged as versatile fluorescent chemosensors, enabling bioimaging of ionic species, reactive oxygen and sulfur species, biomacromolecules and microenvironments (Yin *et al.*, 2020). Synthetic efforts often employ 2,3,4,9-tetrahydrocarbazol-1-ones as precursors, which provide easily accessible intermediates for the construction of diverse heteroannulated carbazoles (*e.g.* Suvarna *et al.*, 2024). In particular, pyrazolo[3,4-*a*]carbazoles bridge the gap between natural carbazole alkaloids and synthetic medicinal chemistry, offering a scaffold of broad medical importance in oncology, infectious disease and neurology (Ramoba *et al.*, 2025; Menezes & Bhat, 2025). As part of our studies in this area, we now describe the synthesis and structure of the title compound 9-methyl-1,10-dihydropyrazolo[3,4-*a*]carbazole, (**I**).

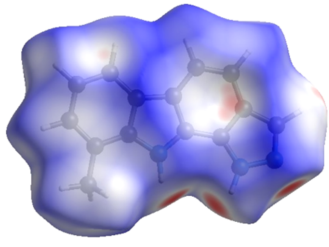

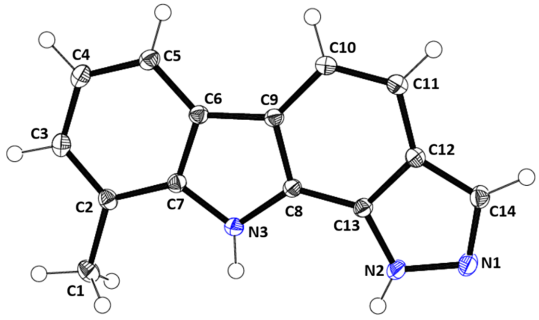

Figure 1
The molecular structure of (**I**), showing displacement ellipsoids drawn at the 50% probability level.

2. Structural commentary

In the solid state, compound (**I**) (Fig. 1) is slightly puckered, the dihedral angle between the outer C2–C7 and N1/N2/C13/C12/C14 rings being 2.24 (7)°. The dihedral angle between the inner C6–C9/N3 and C8–C13 rings is 1.79 (7)°. Alternately, the molecule may be regarded as almost planar, the r.m.s. deviation from planarity for all the C and N atoms being 0.022 Å. Significant bond lengths and angles include C6—C9 [1.447 (2) Å], C11—C12 [1.425 (2) Å], N1—N2 [1.3667 (19) Å], N3—C8—C13 [130.82 (13)°], C13—N2—N1 [111.40 (12)°] and N2—N1—C14 [105.60 (12)°].

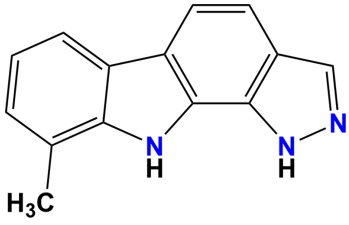

3. Supramolecular features

In the extended structure of (**I**), the molecules are linked by N—H···N hydrogen bonds, with atom N1 accepting two such bonds from both N2—H2 and N3—H3*A* (Table 1 and Fig. 2). This generates an [010] chain, with adjacent molecules in the chain related by a 2_1 screw axis. The packing also exhibits three weak C—H···π interactions that connect parallel chains (Fig. 3 and Table 1). The molecules exhibit some apparent offset π–π stacking interactions with an interplanar spacing of 3.491 Å between molecules related by a translation along the *b* axis. However, a quantitative analysis of these interactions (see *Hirshfeld surface analysis* section below) suggests that they make a very minor contribution to the overall packing of (**I**).

Table 1
Hydrogen-bond geometry (Å, °).

*Cg*1, *Cg*3 and *Cg*4 are the centroids of the N1/N2/C13/C12/C14, C2–C7 and C8–C13 rings, respectively.

D—H···*A*	*D*—H	H···*A*	*D*···*A*	*D*—H···*A*
N2—H2···N1^{i}	0.80 (2)	2.37 (2)	3.097 (2)	150.9 (19)
N3—H3*A*···N1^{i}	0.88 (2)	2.24 (2)	3.050 (2)	152.8 (17)
C1—H1*B*···*Cg*1^{ii}	0.98	2.74	3.504 (3)	135
C5—H5···*Cg*3^{iii}	0.95	2.57	3.408 (3)	147
C14—H14···*Cg*4^{iv}	0.95	2.47	3.264 (3)	142

Symmetry codes: (i) $-x, y+\frac{1}{2}, -z+\frac{1}{2}$; (ii) $x, y+1, z$; (iii) $x+\frac{1}{2}, -y+\frac{1}{2}, -z$; (iv) $-x+1, y-\frac{1}{2}, -z+\frac{1}{2}$.

4. Database survey

A search of the Cambridge Structural Database (CSD, Version 6.01, updated to November 2025; Groom *et al.*, 2016) using the core structure of (**I**) gave one hit, namely, 3,9-dimethyl-1,10-dihydropyrazolo[3,4-*a*]carbazole (CSD refcode TIGPIJ; Martin *et al.*, 2007), in which a methyl group occurs additionally at the 3-position [atom C14 in (**I**)]. The only other compound sharing the same core tetracyclic structure as the

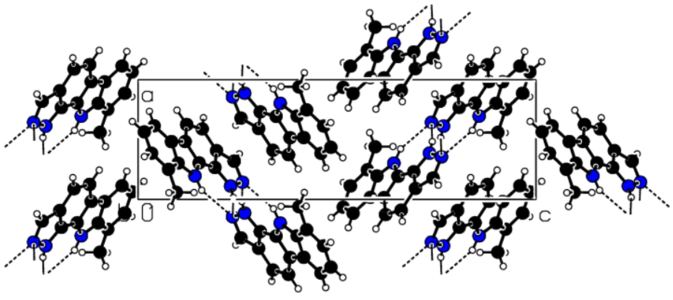

Figure 2
Partial packing view of (**I**), viewed down the *b*-axis direction, showing the hydrogen bonds. Black dashed lines represent N—H···N hydrogen bonds.

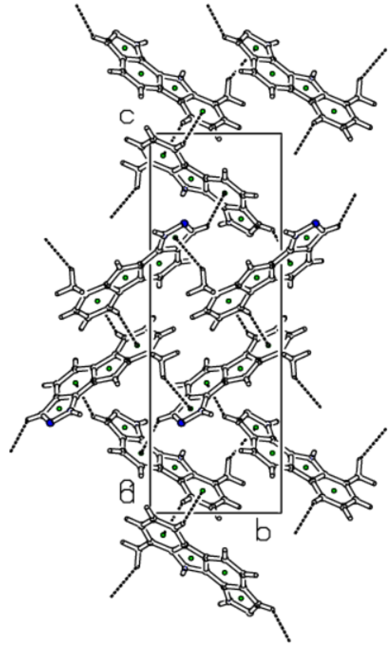

Figure 3
Straw-style packing view of (**I**), viewed down the *a*-axis direction, showing the C—H···π contacts. Centroids are given as green spheres and black dashed lines are H···π contacts.

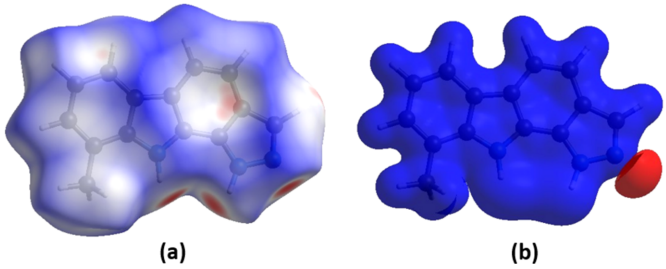

Figure 4
(*a*) View of the three-dimensional Hirshfeld surface of (**I**), plotted over d_{norm} in the range from −0.39 to 1.20 a.u. (*b*) View of the three-dimensional electrostatic potential surface of (**I**) plotted over the range from −0.05 to 0.05 a.u., using the STO-3G basis set at the Hartree–Fock method of theory.

title compound is 7-methyl-1-phenyl-1,10-dihydropyrazolo-[3,4-*a*]carbazole (CSD refcode ZIJGIK), featuring a phenyl substituent at the pyrazole N atom [N2 in (**I**)] and a methyl group at the 7-position [C4 in (**I**)] (Archana *et al.*, 2013).

5. Hirshfeld surface (HS) and 2D fingerprint plots

CrystalExplorer (Version 21.5; Spackman *et al.*, 2021) was used to investigate and visualize further the intermolecular interactions of (**I**). The HS plotted over d_{norm} in the range from −0.39 to 1.20 a.u. is shown in Fig. 4(*a*). The electrostatic potential surface using the STO-3G basis set at the Hartree–Fock level of theory and mapped on the Hirshfeld surface over the range from −0.05 to 0.05 a.u. clearly shows the positions of the close intermolecular contacts in the compound [Fig. 4(*b*)]. The positive electrostatic potential (blue area) over the surface indicates hydrogen-donor potential, whereas the negative (red area) represents the hydrogen-bond acceptors.

The overall two-dimensional fingerprint plot is shown in Fig. 5(*a*), while those delineated into H···H, C···H/H···C, C···N/N···C, N···H/H···N and C···C contacts are illustrated in Figs. 5(*b*)–5(*f*), respectively, together with their relative contributions to the Hirshfeld surface. The most significant interaction type is H···H, contributing 43.1% to the Hirshfeld surface, which is reflected in Fig. 5(*b*) as widely scattered points of high density due to the large hydrogen content of the molecule. In the presence of C···H interactions, the pair of characteristic wings in the fingerprint plot is delineated into C···H/H···C contacts [36.8% contribution to the HS; Fig. 5(*c*)]. The C···N/N···C contacts contribute only 1.5% [Fig. 5(*d*)] and the N···H/H···N contacts contribute 15.3% [Fig. 5(*e*)]. Finally, the C···C contacts [Fig. 5(*f*)] contribute only 3.3%. The packing of (**I**) is thus dominated by van der Waals interactions, augmented by N—H···N hydrogen bonds and some C—H···π interactions, while π–π interactions play only a very minor role, despite the planar nature of the individual molecules.

For a DFT and molecular docking study of (**I**), see the supporting information.

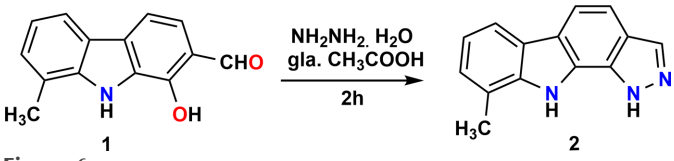

Figure 6
The synthesis of (**I**).

6. Synthesis and crystallization

A solution of 1-hydroxy-8-methyl-9*H*-carbazole-2-carbaldehyde (0.001 mol) in glacial acetic acid (20 ml) was treated with hydrazine hydrate (0.1 ml, 0.002 mol) under continuous stirring. The reaction mixture was subjected to reflux in an oil

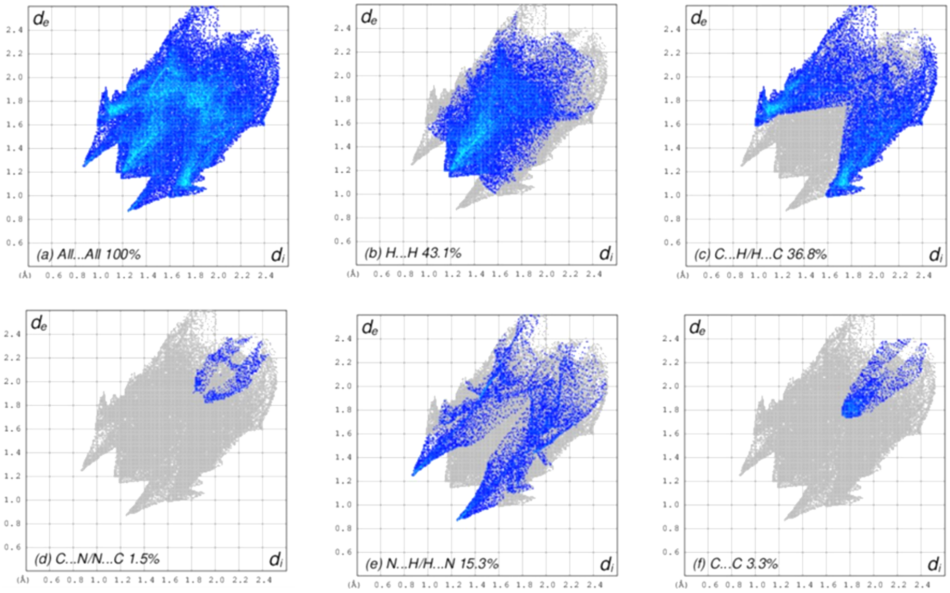

Figure 5
Two-dimensional fingerprint plots for (**I**), showing (*a*) all interactions, and delineated into (*b*) H···H, (*c*) C···H/H···C, (*d*) C···N/N···C, (*e*) N···H/H···N and (*f*) C···C interactions. The d_i and d_e values are the closest internal and external distances (in Å) from given points on the Hirshfeld surface.

bath for 2 h, and the progress of the transformation was monitored periodically by thin-layer chromatography (TLC) using petroleum ether–ethyl acetate (8:2 *v*/*v*) as the mobile phase. Upon completion, the hot reaction mixture was poured onto crushed ice, resulting in the immediate precipitation of a yellow solid. The solid was collected by vacuum filtration, washed thoroughly with distilled water to remove residual acetic acid and air-dried. The crude product was further purified by column chromatography over silica gel, employing petroleum ether–ethyl acetate (90:10 *v*/*v*) as the eluent. This afforded the title compound as a yellow crystalline solid (Fig. 6). Yellow prisms of (**I**) were recrystallized from ethanol solution.

Pale-yellow solid (0.191 g, 86%); m.p. 474–476 K; IR: ν_{max} 3393, 2919, 1619, 1570, 1480, 1228, 1056, 857 cm^{-1}. ^{1}H NMR: δ 12.48 (*b s*, 1H, pyrazole –NH), 11.16 (*s*, 1H, N10-H), 8.16 (*s*, 1H, C3-H), 7.96 (*d*, 1H, C6-H, *J* = 7.56 Hz), 7.82 (*d*, 1H, C4-H, *J* = 8.44 Hz), 7.48 (*d*, 1H, C5-H, *J* = 8.44 Hz), 7.20 (*d*, 1H, C8-H, *J* = 6.88 Hz), 7.12 (*t*, 1H, C7-H, *J* = 7.60 Hz), 2.48 (*s*, 3H, C9-CH_3). MS: *m*/*z* (%) 221 (M^+ = 100). Analysis calculated (%) for $C_{14}H_{11}N_3$: C 76.00, H 5.01, N 18.99; found: C 75.89, H 4.92, N 18.76.

7. Refinement

Crystal data, data collection and structure refinement details are summarized in Table 2. Atoms H2 and H3*A* bonded to N2 and N3 were located in a difference Fourier map and refined isotropically with U_{iso}(H) = 1.2U_{eq}(N). All the other H atoms were placed in calculated positions and were refined with U_{iso}(H) = 1.2U_{eq}(C) or 1.5U_{eq}(methyl C).

Table 2
Experimental details.

Crystal data	
Chemical formula	$C_{14}H_{11}N_3$
M_r	221.26
Crystal system, space group	Orthorhombic, $P2_12_12_1$
Temperature (K)	100
a, *b*, *c* (Å)	6.570 (4), 7.541 (5), 21.854 (14)
V (Å^3)	1082.8 (12)
Z	4
Radiation type	Mo *Kα*
μ (mm^{-1})	0.08
Crystal size (mm)	0.45 × 0.28 × 0.25
Data collection	
Diffractometer	Bruker SMART APEX CCD
Absorption correction	Multi-scan (*SADABS2016*; Krause *et al.*, 2015)
T_{min}, T_{max}	0.714, 0.746
No. of measured, independent and observed [$I > 2\sigma(I)$] reflections	13749, 3671, 3470
R_{int}	0.024
(sin $\theta/\lambda)_{max}$ (Å^{-1})	0.752
Refinement	
$R[F^2 > 2\sigma(F^2)]$, $wR(F^2)$, *S*	0.037, 0.098, 1.05
No. of reflections	3671
No. of parameters	161
H-atom treatment	H atoms treated by a mixture of independent and constrained refinement
$\Delta\rho_{max}$, $\Delta\rho_{min}$ (e Å^{-3})	0.37, −0.25
Absolute structure	Flack *x* determined using 1366 quotients $[(I^+)-(I^-)]/[(I^+)+(I^-)]$ (Parsons *et al.*, 2013)
Absolute structure parameter	0.5 (6)

Computer programs: *APEX2* (Bruker, 2007), *SAINT* (Bruker, 2025), *SHELXS* (Sheldrick, 2008), *SHELXL2025* (Sheldrick, 2015), *PLATON* (Spek, 2020) and *publCIF* (Westrip, 2010).

Acknowledgements

The contributions of the authors are as follows: conceptualization, synthesis, methodology and writing original draft, MS; crystallographic analysis, Hirshfeld surface analysis, molecular docking, software, validation, review and editing, AAT; DFT, software and validation, BMR. MS thanks the academic and administrative authorities of RV College of Engineering for their support and encouragement. The authors thank Dr M. Zeller for the X-ray data collection. The X-ray diffractometer was funded by NSF Grant CHE 0087210, Ohio Board of Regents Grant CAP-491, and by Youngstown State University.

References

Archana, R., Yamuna, E., Thiruvalluvar, A., Rajendra Prasad, K. J., Butcher, R. J., Gupta, S. K. & Öztürk Yildirim, S. (2013). *Acta Cryst.* E**69**, o801.

Bruker (2007). *APEX2*. Bruker AXS Inc., Madison, Wisconsin, USA.

Bruker (2025). *SAINT*. Bruker AXS Inc., Madison, Wisconsin, USA.

El-Essawy, F. A. & Odah, M. A. A. (2024). *ChemistryOpen* **13**, e202400070.

Groom, C. R., Bruno, I. J., Lightfoot, M. P. & Ward, S. C. (2016). *Acta Cryst.* B**72**, 171–179.

Iorkula, T. H., Jude-Kelly Osayawe, O., Odogwu, D. A., Ganiyu, L. O., Faderin, E., Awoyemi, R. F., Akodu, B. O., Ifijen, I. H., Aworinde, O. R., Agyemang, P. & Onyinyechi, O. L. (2025). *RSC Adv.* **15**, 3756–3828.

Knölker, H.-J. & Reddy, K. R. (2002). *Chem. Rev.* **102**, 4303–4427.

Krause, L., Herbst-Irmer, R., Sheldrick, G. M. & Stalke, D. (2015). *J. Appl. Cryst.* **48**, 3–10.

Kumar, M. P., Mahantesh, G., Amaladass, P., Manikandan, C. & Dhayalan, V. (2023). *RSC Adv.* **13**, 32596–32626.

Martin, A. E., Gunaseelan, A. T., Thiruvalluvar, A., Prasad, K. J. R. & Butcher, R. J. (2007). *Acta Cryst.* E**63**, o3471.

Menezes, R. A. & Bhat, K. S. (2025). *Discov. Appl. Sci.* **7**, 137.

Parsons, S., Flack, H. D. & Wagner, T. (2013). *Acta Cryst.* B**69**, 249–259.

Ramoba, L. V., Nzondomyo, W. J., Serala, K., Macharia, L. W., Biswas, S., Prince, S., Malan, F. P., Alexander, O. T. & Manicum, A. E. (2025). *ACS Omega* **10**, 12671–12678.

Sheldrick, G. M. (2008). *Acta Cryst.* A**64**, 112–122.

Sheldrick, G. M. (2015). *Acta Cryst.* C**71**, 3–8.

Spackman, P. R., Turner, M. J., McKinnon, J. J., Wolff, S. K., Grimwood, D. J., Jayatilaka, D. & Spackman, M. A. (2021). *J. Appl. Cryst.* **54**, 1006–1011.

Spek, A. L. (2020). *Acta Cryst.* E**76**, 1–11.

Suvarna, E., Setlur, A. S., Chandrashekar, K., Sridharan, M. & Niranjan, V. (2024). *Comput. Biol. Chem.* **108**, 107979.

Westrip, S. P. (2010). *J. Appl. Cryst.* **43**, 920–925.

Yin, J., Ma, Y., Li, G., Peng, M. & Lin, W. (2020). *Coord. Chem. Rev.* **412**, 213257.

supporting information

Acta Cryst. (2026). E**82**, 231-234 [https://doi.org/10.1107/S2056989026000502]

Synthesis and structure of 9-methyl-1,10-dihydropyrazolo[3,4-*a*]carbazole

M. Sridharan, Aravazhi Amalan Thiruvalluvar and B. M. Rajesh

Computing details

9-Methyl-1,10-dihydropyrazolo[3,4-*a*]carbazole

Crystal data

$C_{14}H_{11}N_3$
M_r = 221.26
Orthorhombic, $P2_12_12_1$
a = 6.570 (4) Å
b = 7.541 (5) Å
c = 21.854 (14) Å
V = 1082.8 (12) Å^3
Z = 4
$F(000)$ = 464
D_x = 1.357 Mg m^{-3}
Melting point: 475(1) K
Mo $K\alpha$ radiation, λ = 0.71073 Å
Cell parameters from 5839 reflections
θ = 2.9–32.2°
μ = 0.08 mm^{-1}
T = 100 K
Prism, yellow
0.45 × 0.28 × 0.25 mm

Data collection

Bruker SMART APEX CCD diffractometer
Radiation source: fine-focus sealed tube
Graphite monochromator
ω scans
Absorption correction: multi-scan (SADABS2016; Krause *et al.*, 2015)
T_{min} = 0.714, T_{max} = 0.746
13749 measured reflections
3671 independent reflections
3470 reflections with $I > 2\sigma(I)$
R_{int} = 0.024
θ_{max} = 32.3°, θ_{min} = 1.9°
h = −9→9
k = −11→10
l = −32→31

Refinement

Refinement on F^2
Least-squares matrix: full
$R[F^2 > 2\sigma(F^2)]$ = 0.037
$wR(F^2)$ = 0.098
S = 1.05
3671 reflections
161 parameters
0 restraints
Primary atom site location: structure-invariant direct methods
Secondary atom site location: difference Fourier map
Hydrogen site location: mixed
H atoms treated by a mixture of independent and constrained refinement
$w = 1/[\sigma^2(F_o^2) + (0.0582P)^2 + 0.1706P]$ where $P = (F_o^2 + 2F_c^2)/3$
$(\Delta/\sigma)_{max}$ < 0.001
$\Delta\rho_{max}$ = 0.37 e Å^{-3}
$\Delta\rho_{min}$ = −0.25 e Å^{-3}
Absolute structure: Flack x determined using 1366 quotients [(I+)-(I-)]/[(I+)+(I-)] (Parsons *et al.*, 2013)
Absolute structure parameter: 0.5 (6)

Special details

Geometry. All esds (except the esd in the dihedral angle between two l.s. planes) are estimated using the full covariance matrix. The cell esds are taken into account individually in the estimation of esds in distances, angles and torsion angles; correlations between esds in cell parameters are only used when they are defined by crystal symmetry. An approximate (isotropic) treatment of cell esds is used for estimating esds involving l.s. planes.

Fractional atomic coordinates and isotropic or equivalent isotropic displacement parameters (Å²)

	x	*y*	*z*	U_{iso}*/U_{eq}
C1	0.0602 (2)	0.5882 (2)	0.09586 (7)	0.0194 (3)
H1A	0.056164	0.706817	0.077613	0.029*
H1B	0.057787	0.598395	0.140561	0.029*
H1C	−0.058266	0.519946	0.082146	0.029*
C2	0.2520 (2)	0.49503 (19)	0.07631 (6)	0.0153 (2)
C3	0.3868 (2)	0.56427 (19)	0.03354 (6)	0.0176 (3)
H3	0.358181	0.676651	0.015884	0.021*
C4	0.5644 (2)	0.47378 (19)	0.01542 (7)	0.0181 (3)
H4	0.651095	0.525425	−0.014452	0.022*
C5	0.6148 (2)	0.31070 (19)	0.04042 (6)	0.0163 (3)
H5	0.735680	0.250830	0.028457	0.020*
C6	0.4828 (2)	0.23636 (18)	0.08385 (6)	0.0139 (2)
C7	0.3035 (2)	0.32869 (18)	0.10041 (6)	0.0141 (2)
C8	0.3057 (2)	0.07438 (18)	0.15330 (6)	0.0135 (2)
C9	0.4842 (2)	0.07220 (17)	0.11814 (6)	0.0138 (2)
C10	0.6257 (2)	−0.07029 (19)	0.12205 (6)	0.0162 (2)
H10	0.745464	−0.068954	0.097703	0.019*
C11	0.5891 (2)	−0.21041 (18)	0.16118 (6)	0.0165 (3)
H11	0.682735	−0.306001	0.164139	0.020*
C12	0.4079 (2)	−0.20876 (18)	0.19703 (6)	0.0144 (2)
C13	0.26791 (19)	−0.06831 (18)	0.19293 (6)	0.0140 (2)
C14	0.3203 (2)	−0.32329 (19)	0.24136 (6)	0.0173 (3)
H14	0.379954	−0.431679	0.254346	0.021*
N1	0.14434 (18)	−0.26063 (18)	0.26256 (6)	0.0195 (2)
N2	0.11285 (18)	−0.10440 (17)	0.23232 (6)	0.0173 (2)
N3	0.19676 (18)	0.22779 (16)	0.14285 (5)	0.0152 (2)
H2	0.017 (3)	−0.042 (3)	0.2393 (9)	0.018*
H3A	0.077 (3)	0.250 (3)	0.1598 (9)	0.018*

Atomic displacement parameters (Å²)

	U^{11}	U^{22}	U^{33}	U^{12}	U^{13}	U^{23}
C1	0.0191 (6)	0.0179 (6)	0.0212 (6)	0.0043 (5)	−0.0022 (5)	0.0003 (5)
C2	0.0175 (6)	0.0139 (6)	0.0146 (5)	0.0009 (5)	−0.0018 (4)	−0.0007 (5)
C3	0.0221 (6)	0.0143 (6)	0.0163 (6)	−0.0018 (5)	−0.0012 (5)	0.0014 (5)
C4	0.0209 (6)	0.0175 (6)	0.0160 (6)	−0.0042 (5)	0.0013 (5)	0.0017 (5)
C5	0.0174 (6)	0.0176 (6)	0.0140 (5)	−0.0013 (5)	0.0017 (5)	0.0001 (5)
C6	0.0145 (5)	0.0144 (5)	0.0129 (5)	0.0000 (4)	0.0009 (4)	−0.0006 (4)
C7	0.0155 (5)	0.0146 (5)	0.0121 (5)	−0.0001 (5)	0.0001 (4)	0.0001 (4)

C8	0.0129 (5)	0.0142 (5)	0.0133 (5)	0.0008 (5)	0.0006 (4)	0.0012 (4)
C9	0.0138 (5)	0.0149 (5)	0.0126 (5)	0.0005 (5)	0.0015 (4)	−0.0003 (5)
C10	0.0150 (5)	0.0166 (6)	0.0168 (6)	0.0019 (5)	0.0025 (5)	−0.0004 (5)
C11	0.0160 (6)	0.0156 (6)	0.0179 (6)	0.0019 (5)	0.0010 (5)	−0.0006 (5)
C12	0.0143 (6)	0.0140 (5)	0.0149 (5)	0.0003 (4)	−0.0008 (4)	−0.0004 (5)
C13	0.0128 (5)	0.0156 (6)	0.0137 (5)	−0.0003 (4)	0.0005 (4)	0.0012 (5)
C14	0.0155 (6)	0.0173 (6)	0.0191 (6)	0.0000 (5)	−0.0012 (5)	0.0042 (5)
N1	0.0170 (5)	0.0205 (6)	0.0210 (6)	−0.0008 (5)	0.0013 (4)	0.0074 (5)
N2	0.0143 (5)	0.0188 (6)	0.0189 (5)	0.0016 (4)	0.0039 (4)	0.0058 (5)
N3	0.0141 (5)	0.0156 (5)	0.0158 (5)	0.0024 (4)	0.0024 (4)	0.0017 (4)

Geometric parameters (Å, º)

C1—C2	1.505 (2)	C8—C9	1.4023 (19)
C1—H1A	0.9800	C8—C13	1.403 (2)
C1—H1B	0.9800	C9—C10	1.424 (2)
C1—H1C	0.9800	C10—C11	1.380 (2)
C2—C3	1.390 (2)	C10—H10	0.9500
C2—C7	1.402 (2)	C11—C12	1.425 (2)
C3—C4	1.408 (2)	C11—H11	0.9500
C3—H3	0.9500	C12—C13	1.4058 (19)
C4—C5	1.386 (2)	C12—C14	1.420 (2)
C4—H4	0.9500	C13—N2	1.3612 (18)
C5—C6	1.4027 (19)	C14—N1	1.3319 (19)
C5—H5	0.9500	C14—H14	0.9500
C6—C7	1.415 (2)	N1—N2	1.3667 (19)
C6—C9	1.447 (2)	N2—H2	0.80 (2)
C7—N3	1.3897 (18)	N3—H3A	0.88 (2)
C8—N3	1.3794 (18)		
C2—C1—H1A	109.5	C9—C8—C13	118.49 (12)
C2—C1—H1B	109.5	C8—C9—C10	121.49 (13)
H1A—C1—H1B	109.5	C8—C9—C6	105.57 (11)
C2—C1—H1C	109.5	C10—C9—C6	132.91 (12)
H1A—C1—H1C	109.5	C11—C10—C9	120.08 (13)
H1B—C1—H1C	109.5	C11—C10—H10	120.0
C3—C2—C7	115.78 (13)	C9—C10—H10	120.0
C3—C2—C1	123.33 (13)	C10—C11—C12	118.65 (12)
C7—C2—C1	120.88 (13)	C10—C11—H11	120.7
C2—C3—C4	122.35 (14)	C12—C11—H11	120.7
C2—C3—H3	118.8	C13—C12—C14	103.67 (12)
C4—C3—H3	118.8	C13—C12—C11	121.21 (12)
C5—C4—C3	121.15 (13)	C14—C12—C11	135.12 (13)
C5—C4—H4	119.4	N2—C13—C8	132.52 (13)
C3—C4—H4	119.4	N2—C13—C12	107.39 (12)
C4—C5—C6	118.25 (13)	C8—C13—C12	120.09 (12)
C4—C5—H5	120.9	N1—C14—C12	111.94 (13)
C6—C5—H5	120.9	N1—C14—H14	124.0

C5—C6—C7	119.42 (13)	C12—C14—H14	124.0
C5—C6—C9	133.50 (13)	C14—N1—N2	105.60 (12)
C7—C6—C9	107.07 (11)	C13—N2—N1	111.40 (12)
N3—C7—C2	128.21 (13)	C13—N2—H2	126.2 (14)
N3—C7—C6	108.76 (12)	N1—N2—H2	122.3 (14)
C2—C7—C6	123.03 (13)	C8—N3—C7	107.93 (12)
N3—C8—C9	110.67 (12)	C8—N3—H3A	123.4 (13)
N3—C8—C13	130.82 (13)	C7—N3—H3A	128.6 (13)
C7—C2—C3—C4	−0.1 (2)	C6—C9—C10—C11	177.71 (14)
C1—C2—C3—C4	−179.28 (13)	C9—C10—C11—C12	0.1 (2)
C2—C3—C4—C5	−1.0 (2)	C10—C11—C12—C13	0.2 (2)
C3—C4—C5—C6	0.8 (2)	C10—C11—C12—C14	−179.27 (15)
C4—C5—C6—C7	0.31 (19)	N3—C8—C13—N2	1.7 (3)
C4—C5—C6—C9	179.06 (14)	C9—C8—C13—N2	179.72 (14)
C3—C2—C7—N3	−179.06 (14)	N3—C8—C13—C12	−177.62 (14)
C1—C2—C7—N3	0.2 (2)	C9—C8—C13—C12	0.36 (19)
C3—C2—C7—C6	1.26 (19)	C14—C12—C13—N2	−0.32 (15)
C1—C2—C7—C6	−179.52 (13)	C11—C12—C13—N2	−179.92 (13)
C5—C6—C7—N3	178.86 (12)	C14—C12—C13—C8	179.19 (12)
C9—C6—C7—N3	−0.19 (15)	C11—C12—C13—C8	−0.4 (2)
C5—C6—C7—C2	−1.4 (2)	C13—C12—C14—N1	0.00 (16)
C9—C6—C7—C2	179.54 (12)	C11—C12—C14—N1	179.52 (15)
N3—C8—C9—C10	178.28 (12)	C12—C14—N1—N2	0.32 (16)
C13—C8—C9—C10	−0.1 (2)	C8—C13—N2—N1	−178.88 (14)
N3—C8—C9—C6	−0.09 (15)	C12—C13—N2—N1	0.54 (16)
C13—C8—C9—C6	−178.45 (12)	C14—N1—N2—C13	−0.53 (16)
C5—C6—C9—C8	−178.69 (15)	C9—C8—N3—C7	−0.02 (15)
C7—C6—C9—C8	0.17 (14)	C13—C8—N3—C7	178.07 (14)
C5—C6—C9—C10	3.2 (3)	C2—C7—N3—C8	−179.58 (13)
C7—C6—C9—C10	−177.93 (14)	C6—C7—N3—C8	0.13 (15)
C8—C9—C10—C11	−0.1 (2)		

Hydrogen-bond geometry (Å, º)

Cg1, Cg3 and Cg4 are the centroids of the N1/N2/C13/C12/C14, C2–C7 and C8–C13 rings respectively.

D—H···*A*	*D*—H	H···*A*	*D*···*A*	*D*—H···*A*
N2—H2···N1^{i}	0.80 (2)	2.37 (2)	3.097 (2)	150.9 (19)
N3—H3*A*···N1^{i}	0.88 (2)	2.24 (2)	3.050 (2)	152.8 (17)
C1—H1*B*···*Cg*1^{ii}	0.98	2.74	3.504 (3)	135
C5—H5···*Cg*3^{iii}	0.95	2.57	3.408 (3)	147
C14—H14···*Cg*4^{iv}	0.95	2.47	3.264 (3)	142

Symmetry codes: (i) −*x*, *y*+1/2, −*z*+1/2; (ii) *x*, *y*+1, *z*; (iii) *x*+1/2, −*y*+1/2, −*z*; (iv) −*x*+1, *y*−1/2, −*z*+1/2.